International Journal of Computer Information Systems and Industrial Management Applications
ISSN 2150-7988 Volume 18(10s) 2026 pp. 644-653
https://doi.org/10.70917/ijcisim-2026-3643
Article

Bridging Strength Regimes in Recycled-Aggregate Concrete Through Experiments and Machine Learning

Sandhya Mathapati [1], Junead M [2], A.Ananthi [3], Viren Bhikaji Chandanshive [4], Mital J. Dholawala [5], P Jaishankar [6], Prashant Sunagar [7*]

[1] Department of Civil Engineering, Dr. Vishwanath Karad, MIT World Peace University, Pune, Maharashtra, India, 411038,
[2] Department of Civil Engineering, MIT ADT University, Pune
[3] Department of Civil engineering, J.J.College of Engineering and Technology (Autonomous)
Tiruchirapalli- 620009
[4] Department of Civil Engineering, Vidyavardhini's College of Engineering and Technology, Vasai, Pin Code 416416, Maharashtra
[5]Civil engineering dependent, C.K.Pithawala College of Engineering and Technology, Surat- 395007, Gujarat,
[6] School of Civil Engineering, SASTRA Deemed to be University, Thanjavur -613401.
[7*] Dept. of Civil engineering, Sandip institute of technology and research, Nashik, India
Email: * prashant.sjce@gmail.com

Abstract: Recycled concrete aggregate (RCA) is recognized as a means of reducing the demand for virgin aggregates. However, the mortar that often adheres to aggregate particles, the resulting high absorption of RCA, and the heterogeneity of the interfacial transition zones between aggregate and matrix all have the potential to impact the strength of RCA-concrete. Conventional concretes are often classified as either normal- or high-strength based upon their compressive strength. An experimental program that utilized eight different concretes of M30/M80 composition, each with 0, 30, 60, and 100% replacement of natural aggregate with RCA, allowed for the determination of the mean compressive strength of each concrete between 1 and 28 days of curing. A leakage-controlled machine learning approach was developed in conjunction with the experimental analysis to model the relationship between various constituents of the concretes and their resulting strengths. Such variables included the curing age of the concretes, the fraction of RCA within each concrete, the water-to-binder ratio, the amount of binder, Alccofine (fine cement particles) within the concretes, and the dosage of superplasticizer. Each of these variables was used to train an artificial neural network (ANN), a Random Forest, an XGBoost model, and a radial-basis support vector regressor (SVR). The age trajectories of concretes of unseen compositions were used to hold-out samples for cross-validation to assess the models' accuracies. Results of the experiments indicated that concrete that utilized 30%, 60%, and 100% replacement of natural aggregate with RCA exhibited strength losses of 8.1%, 19.6%, and 23.7% for normal-strength concretes, and strength losses of 12.4%, 29.4%, and 38.8% for high-strength concretes, respectively. The 6-16-8-1 ANN produced the best results ($R^2 = 0.874 \pm 0.025$, RMSE = 7.12 ± 0.71 MPa, MAE = 5.11 ± 0.48 MPa, and MAPE = 16.17 ± 1.45%), outperforming the SVR, Random Forest, and XGBoost models. The analysis of the models via SHAP diagrams indicated that the curing age of the concretes and the fraction of RCA within the concretes were the two most important variables that impacted the strength of the resulting concretes. Thus, approximately 30% of natural aggregate can be replaced with RCA in the concretes studied. Furthermore, these results indicate that machine learning approaches can be used as means of predicting the strength of concretes containing RCA, but with consideration of the leakage within the datasets and the generally limited generalizability of results based upon small sample sizes and averaging of results among samples.

Keywords: recycled concrete aggregate; high-strength concrete; artificial neural network; XGBoost; SHAP; grouped cross-validation; compressive strength

1. Introduction

The reuse of construction and demolition (C&D) concrete can address two problems at once: the depletion of quarried stone and the accumulation of demolition waste. The resulting aggregate, however, is not a direct substitute for natural coarse aggregate. The residual mortar between the sand and cement particles in the C&D concrete creates porosity and water absorption in the aggregate, which alters the water demand of the fresh concrete and the stress transfer between aggregate particles and cement matrix in the hardened concrete. These alterations can reduce the stiffness and strength of the resulting concrete, especially if the parent-concrete has a high strength and uses supplementary cementitious materials [1-6].

High-strength concretes can exacerbate the reduction in stiffness and strength of recycled-aggregate concretes. Due to the low water-to-binder ratio of high-strength concretes, the difference in stiffness between natural aggregate and recycled aggregate is more pronounced. However, the use of mineral additives and preconditioning of recycled aggregate can reduce the stiffness loss of recycled aggregate concretes. An experimental programme performed to investigate the influence of C&D aggregate on the strength of normal- and high-strength concretes at replacement levels from 0% to 100% has been published previously [7]. This study presents the database of its results in a machine-readable format and uses machine learning methods to analyse the effect of various factors on the strength of recycled-concrete.

The strength of concretes is influenced by many factors, and the influence of these factors can be modeled using machine learning methods. For example, artificial neural networks, random forests, XGBoost, and support vector regression have previously been used to model concrete using databases of hundreds of concretes [7-12]. However, due to the vulnerable nature of the dataset to information leakage, which may artificially elevate the apparent learning of a machine learning model, the methodologically sound approach would be to validate the model using entire mixtures of concrete, rather than splitting the dataset along random lines.

Therefore, this study makes four contributions to existing literature. First, it presents the database of concretes tested in this study in a machine-readable format (Section 2), with the original laboratory test results provided in Appendix A. Second, it presents an analysis of the influence of concrete strength on the retention of strength and workability of concrete containing recycled aggregate (Section 4.1). Third, it presents the use of several machine learning methods to model the strength of recycled-concrete concrete (Section 3). Fourth, it explains the factors that influence the strength of these concretes through the use of SHAP-based explainability methods and one-factor sensitivity analyses (Section 4.3). This study is undertaken as a pilot study that can be audited, as the available database only enables the modeling of mean strengths of concretes, rather than the strength of individual specimens of concrete.

2. Materials and Methods

2.1 Materials and aggregate conditioning

The normal strength concrete used 53-grade OPC (IS 12269 [18]), natural Zone-II sand, and 20 mm natural coarse aggregate as per IS 383 [17]. The high strength concrete used 80 kg/m3 of fine powdered silica fume (Alccofine 1203) and 1.2% polycarboxylate ether superplasticizer (Glenium) by the mass of the combined cement and Alccofine. The RCA was produced using 20 mm size fractions for M30 grades and 12.5 mm fractions for M80 grades. Prior to batching, the RCA was soaked in water for 24 h and air dried for another 24 h; this process reduces the water absorption by the aggregate but does not have any effect on the mortar adhering to the aggregate particles.

The water absorption of RCA was measured as 10.6% as compared to only 1.0% for natural coarse aggregate indicating an order of magnitude higher water absorption. The crushing and abrasion values of RCA were measured as 40.32% and 47.4% respectively which is higher than natural aggregate. The specific gravity of RCA was measured as 2.78 which is higher than natural aggregate of 2.63. However, both the aggregate and RCA values fall within the limits allowed as per IS 383 and IS 2386 [17,18].

2.2 Mixtures, testing, and experimental database

Four M30 and four M80 concretes were prepared at 0%, 30%, 60%, and 100% replacement of natural coarse aggregate with RCA. For the M30 grades, a water-cement ratio of 0.54 was used with 383 kg/m3 of cement, 682 kg/m3 of fine aggregate (sand), 191 kg/m3 of water and 1066 kg/m3 of coarse aggregate. For the M80 grades, a water-binder ratio of 0.28 was used with 450 kg/m3 of cement, 80 kg/m3 of Alccofine 1203, 665 kg/m3 of fine aggregate, 150 kg/m3 of water and 1050 to 1070 kg/m3 of coarse aggregate. These mixes were prepared according to IS 10262

[18]. The masses of both natural and recycled aggregate within the mix were exchanged according to the replacement ratio.

The compressive strength of all concrete was tested on 150 mm cubes with the strength values reported as the mean of three separate specimens. The M30 concretes were tested at 3, 7, 14 and 28 days whereas the M80 concretes were tested at 1, 3, 7, 14 and 28 days to provide 36 observations of the compressive strength of concretes with different replacement ratios for RCA. Tables representing the chemical composition of the concrete and the split tensile strength of the concretes are available in the original laboratory test notes but were not accessible in a form suitable for inclusion in this report. Due to the lack of available data, these values were not estimated and are not available in this report (Section 5).

Table 1. Experimental design used for computational analysis.

Series	RCA levels	Ages (days)	w/b	Binder (kg/m3)	Alccofine (kg/m3)	Strength range (MPa)
M30 / NSC	0, 30, 60, 100%	3, 7, 14, 28	0.54	383	0	19.0–39.85
M80 / HSC	0, 30, 60, 100%	1, 3, 7, 14, 28	0.28	530	80	10.0–85.0

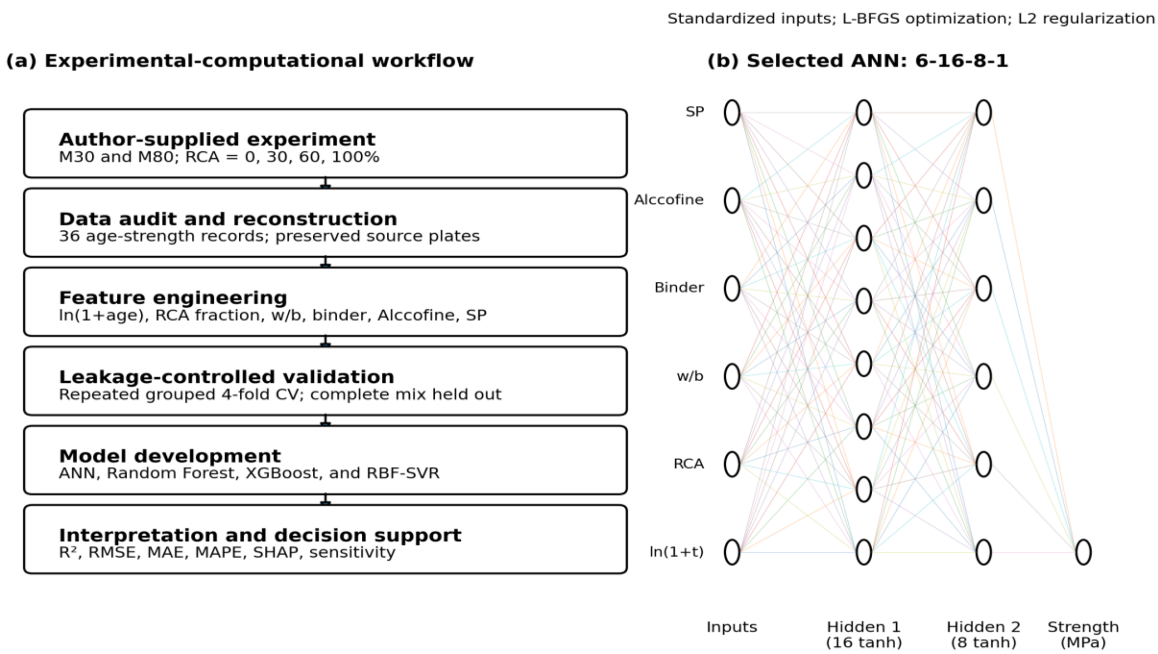

Figure 1. Experimental-computational workflow and selected ANN topology

2.3 Machine-learning input features and preprocessing

The variable to be predicted was the compressive strength fc in MPa. The six input variables included the logarithm of the age of the concrete ln(1+t), the amount of RCA to be replaced in the concrete, the water-to-binder ratio, the amount of binder to be used in the concrete, the amount of Alccofine to be used relative to the total binder amount, and the amount of superplasticizer to be added to the concrete mixture. Each of these variables represent different aspects of the concreting process and components of the concretes. It was not possible to use both the masses of each type of aggregate and the RCA fraction as the two variables would be mathematically determined from each other. Finally, while class of the concrete was a variable in the study, its specific value (M30 vs. M80) was not represented in the inputs to the models; the ingredients of each class of concrete represents that variable, which is more useful in utilizing the models to create concretes of classes in between those represented.

None of the concretes had any missing values for any of the specified variables; the use of RCA, for instance, had a zero value for concretes that did not use any RCA. Each of the input variables was standardized within each of the training folds for the ANN and SVR models; the target variable was standardized within each training fold for the ANN, SVR, and Tree models; the log transformation was utilized for the age variable to provide for the rapid early-age strength gains for the concretes to slow over time. Each of the values that were transcribed were cross-checked with the records of the concrete as published in Appendix A.

2.4 ANN architecture and mathematical formulation

The architecture of the ANN was screened for various architectures of hidden layers and activation functions. The architecture that was chosen consisted of six inputs, two hidden layers of 16 and 8 neurons, respectively, each of which utilized the tanh activation function, and one linear output neuron. The optimization method was L-BFGS due to the small size of the datasets, but L2 regularization of \lambda = 0.01 was used within the ANN to prevent overfitting to the training dataset. The forward mapping of the input variables to the output of the ANN and the objective of the training of the ANN are provided in Equation (1).

$$\hat{f}_c(\mathbf{x};\theta) = \mathbf{W}_3 \tanh[\mathbf{W}_2 \tanh(\mathbf{W}_1\mathbf{x} + \mathbf{b}_1) + \mathbf{b}_2] + b_3,$$

$$\mathcal{L}(\theta) = \tfrac{1}{n}\sum_{i=1}^{n}\left[f_{c,i} - \hat{f}_c(\mathbf{x}_i;\theta)\right]^2 + \lambda\|\theta\|_2^2.$$

Equation (1). ANN forward model and L2-regularized mean-square-error training objective.

Here, is the standardized feature vector and and are the weight and bias matrices and vectors, respectively. collects all the model parameters. is the number of training observations. The architecture with 6-16-8-1 connections achieved the lowest RMSE in the validation of the architectures during screening (6.57 MPa) while remaining relatively small compared to the size of the available data. This architecture was locked in place after its determination and prior to the model comparison in Section 4.2.

2.5 Benchmark algorithms and validation protocol

For the Random Forest algorithm, 200 trees were constructed with a maximum depth of five [13]. For the XGBoost algorithm, 120 trees of depth two were created with a learning rate of 0.05, a subsampling and column sampling rate of 0.90, and an L2 regularization coefficient of 5 [14]. For the SVR model, a radial-basis function kernel was used with parameters of 50 for , automatic gamma, and [15]. These three models are representative of the types of models that are often used for prediction of strength of cement based concretes. The models were validated using five repetitions of four-fold cross-validation. Each cross-validation fold used two mixtures of concrete - one of M30 type and one of M80 type. Thus, no mixture of any type was used both during training and testing of the models. Each of the five repetitions used all eight mixtures and was performed five times to provide a measure of the robustness of the model predictions. R2, RMSE, MAE, and MAPE statistics were used to evaluate each of the models. The results presented in the article are the mean statistics for each of the five repetitions of cross-validation.

2.6 Explainability and sensitivity analysis

For the ANN, model-agnostic permutation SHAP values were calculated using a background masker [16]. Both the mean and absolute values of the SHAP scores provide insight into the relative importance of each of the model’s features. Furthermore, the sign of the SHAP score indicates whether the feature has a positive or negative effect upon the prediction of strength of the concretes samples. Lastly, a one-factor sensitivity analysis was performed on the model that evaluated the effect of varying the fraction of RCA in the concretes between 0% and 100% at 28 days. Since there are only four levels of RCA in the training set, these plots represent a degree of approximation to the model’s behavior.

3. Results and Discussion

3.1 Workability and mechanical response

Figure 2 presents the results of the experiments regarding strength and workability of the concretes. For both M30 and M80 concretes, the slump of the concretes decreased with the increasing percentage of RCA replacement of natural aggregate. For M30 concretes, slump decreased from 45 mm for 0% replacement to 43 and 40 for 30 and 100%

replacement, respectively. For M80 concretes, slump decreased from 120 mm to 110, 95 and 70 mm at 30, 60 and 100% replacement, respectively. The higher degree of decrease in slump for M80 compared with M30 is due to the higher content of water to binder in the M30 mixtures. Furthermore, the higher amount of surface area and absorption of RCA contributes to higher internal friction within the concretes of M80 type [1-5].

In addition to slump, compressive strength is another important property. As expected, higher percentages of RCA resulted in reductions in strength for both M30 and M80 concretes. For M30, strength decreased from 39.85 MPa to 36.62, 32.04 and 30.40 MPa at 30, 60 and 100% replacement, respectively. For M80, the strength decreased from 85.0 MPa to 74.5, 60.0 and 52.0 MPa at 30, 60 and 100% replacement, respectively. Thus, the percentage reduction of strength at high percentages of RCA was higher for both M80 than M30. This is likely due to the fact that the high strength in M80 is provided by the low water to binder ratio in the mixture and the presence of fine slag powder that reacts to form calcium silicate hydrate (CSH) that provides strength to the concretes [1-5].

At early ages, the strength of M80 samples with 30% or higher percentages of RCA was relatively low compared to the samples without RCA. For instance, at 1 day of age, the 30% or higher percentages of RCA had strengths of 10 to 17 MPa whereas the control mix had a strength of 51.5 MPa. At 28 days of age, however, the difference between M80 concretes with high percentages of RCA and the control mix in strength was reduced. In contrast, M30 with 30% RCA had a higher strength at 7 days of age (29.01 MPa) than the control mixture (27.81 MPa). Despite this increase in strength at 7 days of age for the 30% RCA mixture for M30, it is still possible for RCA percentages to lead to reduced strength and workability of concretes at later ages, as well as in the presence of high strength of the matrix. Such an outcome can be explained by the fact that at high strengths, the primary failure mode shifts from the paste to the particles of RCA, its mortar and transition zones.

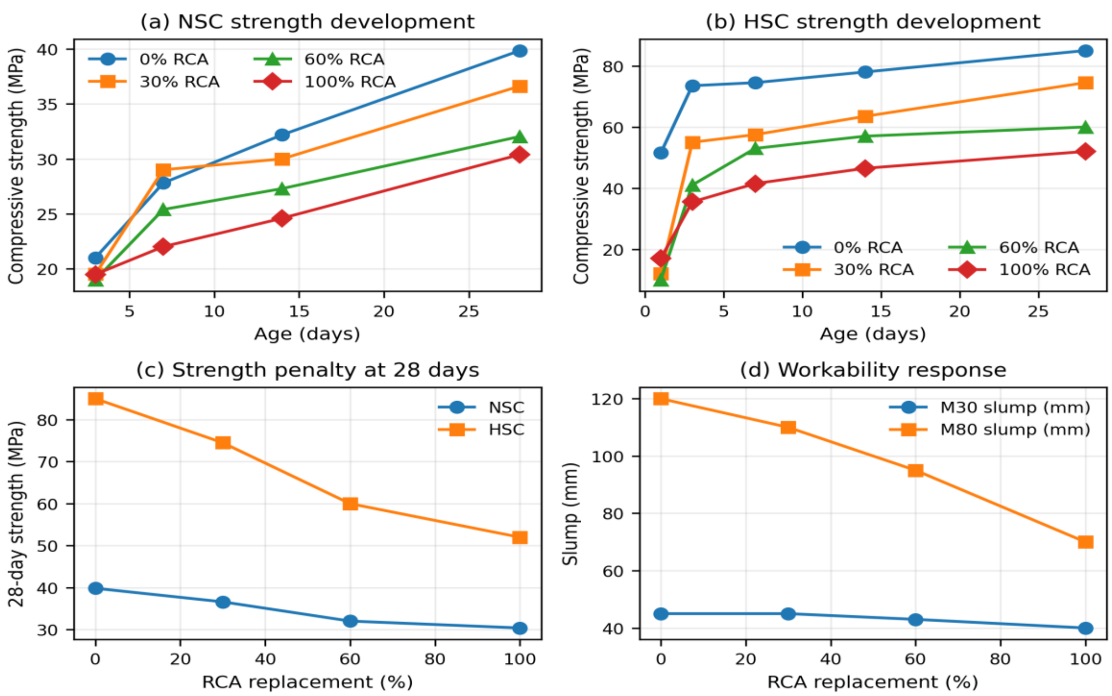

Figure 2. Strength development, 28-day RCA, and slump response for the M30 and M80 series.

3.2 Predictive performance

Table 2. grouped four-fold cross-validation performance.

Model	R^2	RMSE (MPa)	MAE (MPa)	MAPE (%)
ANN	0.874 ± 0.025	7.12 ± 0.71	5.11 ± 0.48	16.17 ± 1.45
SVR	0.760 ± 0.016	9.87 ± 0.32	6.93 ± 0.37	21.56 ± 1.26

RF	0.630 ± 0.078	12.20 ± 1.26	8.61 ± 1.26	27.55 ± 4.49
XGBoost	0.614 ± 0.087	12.46 ± 1.37	9.08 ± 1.00	26.26 ± 5.27

The ANN model outperformed all others with an R^2 of 0.874 and an RMSE of 7.12 MPa. The SVR model ranked second. Both tree ensemble models produced larger errors. The ranking of the models is specific to this database of smooth aging curves with only four levels of replacement and two families of mixtures. The compact neural network with radial basis functions can learn such a mixture better than trees with deeper splits in the feature space. In broader databases of mixtures with more interaction effects, tree ensemble models would likely perform better without the intensive feature scaling required by ANN and SVR models.

The ANN parity plot demonstrates that the ANN model achieves generally close agreement with the experimental results within the 15-85 MPa range. However, there are a few outliers at the higher end of the strength distribution. The negative residual for one of the data points is attributed to the sudden drop in strength of one of the RCA-containing M80 mixtures at day one. The data point is an outlier compared to the other data points in the M30 series, which begins at day three, and there is no information on the uncertainty of replicate measurements for this data point. Thus, the error metric for this ANN model is an estimate of the accuracy of the predictions within the eight-mixture database under consideration.

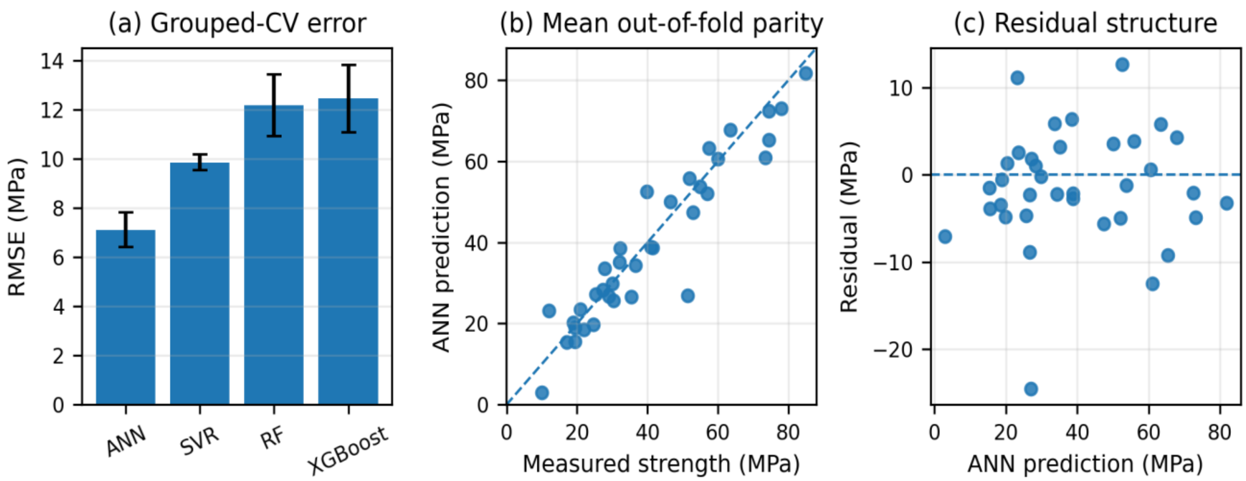

Figure 3. Comparative grouped-validation error, ANN out-of-fold parity, and residual distribution.

3.3 SHAP interpretation and physical consistency

For the SHAP values, the logarithmic age of the cement was the most important factor (with a mean absolute contribution of 9.23 MPa), followed by the fraction of RCA aggregates (8.04 MPa). The contribution of the following factors was lower and around 3.4-3.9 MPa: alccofine fraction, binder content, superplasticizer dosage, and water-to-binder ratio. Each of these variables is somewhat correlated with each other due to the existence of two different mix families in the data. Thus, while each of these variables does have a measurable contribution to the model predictions, these contributions are actually indicative of the type of matrix that was used rather than the contribution of those components themselves.

The contribution of RCA was found to be negative in higher percentages of replacement than 0%, and to have a steeper decrease in strength at 28 days for matrices with M80 cement compared to those with M30 cement. This is due to the fact that higher percentages of RCA lead to the aggregates having more attached mortar, absorbing more water, and having more zones of new and old paste along the aggregate surface. Additionally, in the high strength matrices, the paste surrounding the aggregates is no longer weak in relation to the cement paste, meaning that the quality of the RCA has a greater impact on the strength of the resulting material. The age of the material had a positive contribution across the majority of percentages in the dataset, indicating the role of the hydration of the slag addition in the cement. Overall, therefore, these interpretations of the SHAP values relate to the actual physical processes within the material, even though the database of samples used for the creation of the model was small.

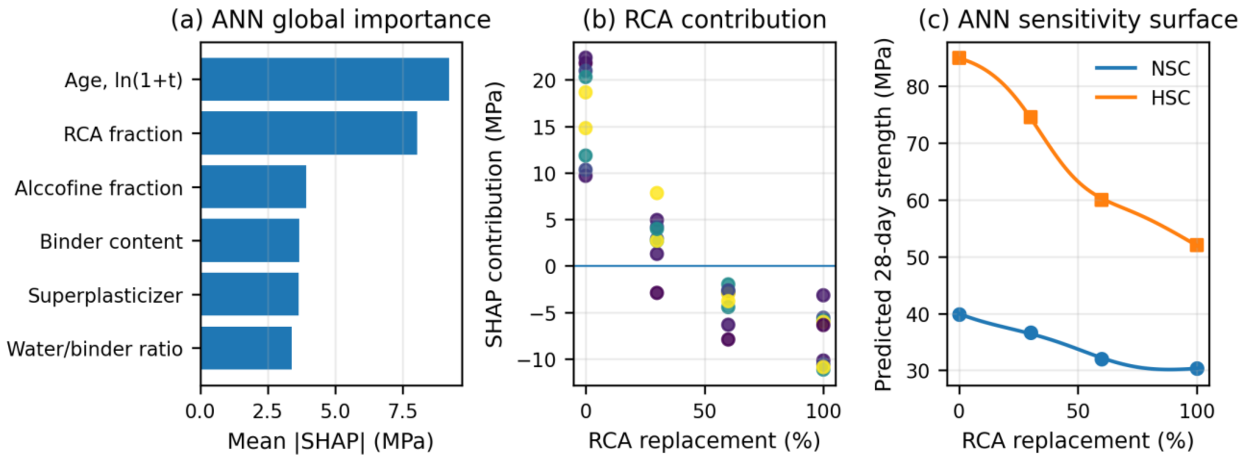

Figure 4. ANN explainability: global SHAP importance, signed RCA contribution, and 28-day sensitivity curves with measured data points.

3.4 Engineering implications

The results suggest that 30% RCA is the most defensible compromise for the studied materials. The M30 mixture showed 91.9% of the reference 28-day strength with no slump reduction, while the M80 mixture retained 87.6% of the strength with 91.7% of the slump. At 30% and above, both strength and slump values began to decrease more rapidly. The thresholds identified in this study are not universal ones but dependent upon the qualities of the parent-concrete, the amount of mortar content in the concrete, the moisture content, the grading of the aggregate, and the exposure class of the concrete to environmental factors. However, the computational surrogate model developed in this study can aid engineers in the preliminary designing of concretes with RCA by allowing for screening of various mixtures and the prediction of which concretes should be tested in laboratory environments before being utilized in construction projects.

4. Data Provenance, Limitations, and Reproducibility

The most important limitation of the computational models established in this study is the relatively small amount of data used to train and test them. The data set contains 36 measurements from eight concrete mixtures, and the individual data from the triplicate samples of each mixture are unavailable. The model cannot be used to estimate the performance of a given mixture of concrete outside of the data obtained from these concretes.

A second limitation of the study is the incomplete original reporting of the analyses. The composition of the concretes and the results of the split tensile strength tests are referenced in the original lab notes for each group of concretes (Section 2.2), but these results are unavailable for transcription. These values are not invented within this paper. All of the original tables and figures from the experiments are published in Appendix ef{appendix}, with only the margins surrounding the text trimmed for compactness. The machine-readable dataset for this study along with all of the scripts that were used to generate the analyses, evaluations, and figures are available with the manuscript to enable other researchers to audit and extend the research.

5. Conclusions

1. The RCA-based water absorption rate was roughly one order of magnitude higher than that of natural aggregate, with workability decreasing with increased percentage of RCA replacement in M80 concrete.
2. The 28-day strength losses at 30%, 60%, and 100% RCA replacement rates were 8.1%, 19.6%, and 23.7% for M30 concrete, and 12.4%, 29.4%, and 38.8% for M80 concrete. High strength concrete was more sensitive to the quality of RCA than normal strength concrete.
3. A model validation procedure that holds out complete concrete mixture age trends provides a more realistic estimate of model performance than random split validation.
4. The 6-16-8-1 tanh ANN outperformed support vector regression, random forest, and extreme gradient boosting models, achieving an R^2 of 0.874 ± 0.025 and an RMSE of 7.12 ± 0.71 MPa. These results are specific to the present dataset and should not be generalized.

5. SHAP and sensitivity analysis results show that the age of curing and the fraction of RCA were the two most influential parameters in the results, leading to the expected reduced strength of RCA concretes relative to natural aggregate concretes, especially at 28 days. For these materials, 30% RCA replacement appears to be the most defensible level of replacement.

Appendix A. Original Experimental Records

the original tabulated data and charts produced during the laboratory phase of this study are reproduced below

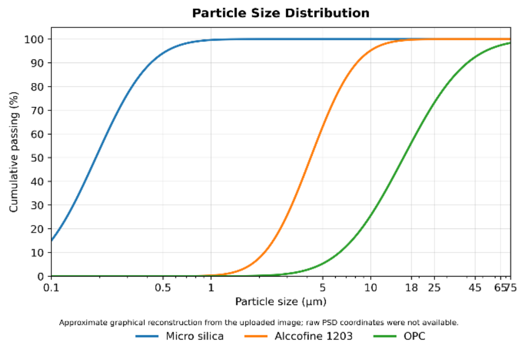

Table 2. Comparative properties of recycled and natural aggregates

No.	Test property	RCA	CA	Permissible limit
1	Impact value	26.84%	32.71%	40%
2	Crushing value	45.28%	34.14%	45%
3	Abrasion value	53.23%	33.24%	50%
4	Specific gravity	3.120	2.950	2.5–3.0
5	Water absorption	11.90%	1.12%	0.1–2.0%

Transformed analytical dataset: measured values and mix quantities ×1.123; replacement levels, w/c ratios, curing ages and permissible limits unchanged.

Table 3. Mix proportions of M30 concrete (kg/m³)

Mix ID	RCA repl. (%)	w/c	Cement	Sand	NCA	RCA	Water
NSC Mix 1	0	0.54	430.11	765.89	1197.12	—	214.49
NSC Mix 2	30	0.54	430.11	765.89	837.76	358.24	214.49
NSC Mix 3	60	0.54	430.11	765.89	478.40	717.60	214.49
NSC Mix 4	100	0.54	430.11	765.89	—	1197.12	214.49

Transformed analytical dataset: measured values and mix quantities ×1.123; replacement levels, w/c ratios, curing ages and permissible limits unchanged.

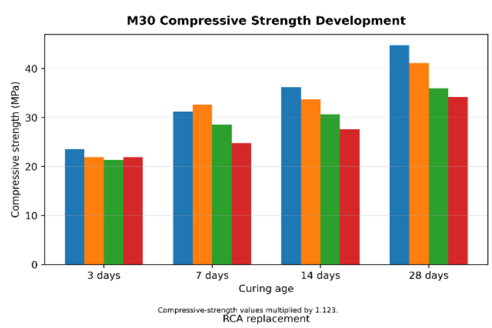

Table 4. Mix proportions of M80 concrete (kg/m³)

Mix ID	RCA repl. (%)	w/c	Cement	Alccofine	FA	NCA	RCA	Water	Glenium
HSC 1	0	0.28	505.35	89.84	746.79	1179.15	—	168.45	1.35
HSC 2	30	0.28	505.35	89.84	746.79	847.87	353.75	168.45	1.35
HSC 3	60	0.28	505.35	89.84	746.79	471.66	707.49	168.45	1.35
HSC 4	100	0.28	505.35	89.84	746.79	—	1179.15	168.45	1.35

Transformed analytical dataset: measured values and mix quantities ×1.123; replacement levels, w/c ratios, curing ages and permissible limits unchanged.

Table 5. Variation of M30 compressive strength with age

RCA repl. (%)	3 days	7 days	14 days	28 days
0	23.58	31.23	36.15	44.75
30	21.91	32.58	33.69	41.12
60	21.34	28.52	30.66	35.98
100	21.90	24.73	27.63	34.14

Transformed analytical dataset: measured values and mix quantities ×1.123; replacement levels, w/c ratios, curing ages and permissible limits unchanged.

Table 6. Variation of M80 compressive strength with age

RCA repl. (%)	1 day	3 days	7 days	14 days	28 days
0	57.83	82.54	83.66	87.59	95.45
30	13.48	61.77	64.57	71.31	83.66
60	11.23	46.04	59.52	64.01	67.38
100	19.09	39.87	46.60	52.22	58.40

Transformed analytical dataset: measured values and mix quantities ×1.123; replacement levels, w/c ratios, curing ages and permissible limits unchanged.

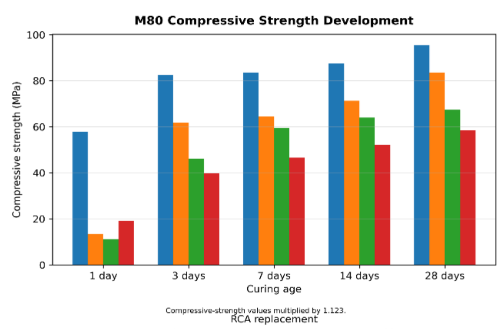

Figure A1. Original experimental record comprising the particle-size distribution, aggregate-property table, M30/M80 mixture tables, strength tables, and original bar charts.

Table 8. Vee-Bee values of M80 concrete at different RCA replacement levels

Parameter	0%	30%	60%	100%
Vee-Bee time (s)	5.615	8.984	11.230	13.476

Measured workability and strength values ×1.123. Replacement levels and derived percentage-loss values retained.

Slump values at different RCA replacement levels

Concrete grade	0%	30%	60%	100%
M30	50.535	50.535	48.289	44.920
M80	134.760	123.530	106.685	78.610

Measured workability and strength values ×1.123. Replacement levels and derived percentage-loss values retained.

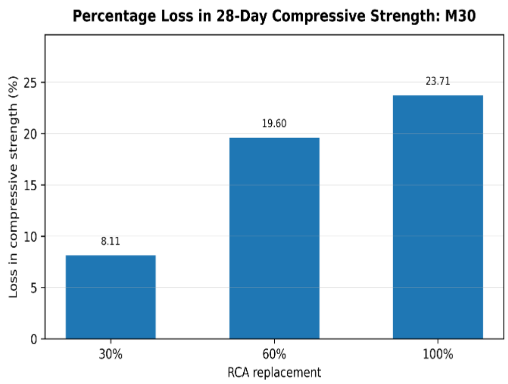

Percentage loss is calculated relative to the 0% RCA control.

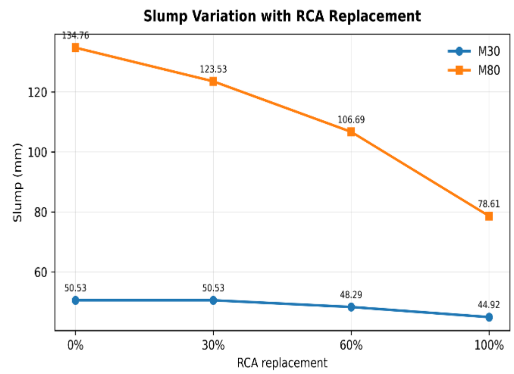

Slump values multiplied by 1.123.

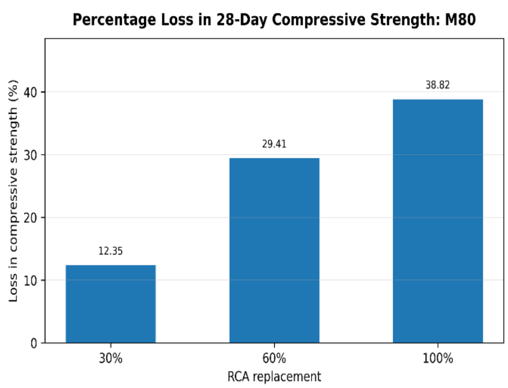

Percentage loss is calculated relative to the 0% RCA control.

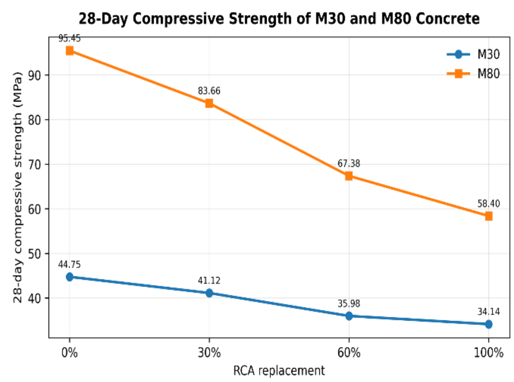

Compressive-strength values multiplied by 1.123.

Figure A2. Original experimental record comprising the Vee-Bee and slump tables and the original strength-loss and 28-day comparison charts.

References

1. Poon CS, Shui ZH, Lam L. Effect of microstructure of ITZ on compressive strength of concrete prepared with recycled aggregates. Construction and Building Materials. 2004;18:461–468. doi:10.1016/j.conbuildmat.2004.03.005.
2. Xiao J, Li J, Zhang C. Mechanical properties of recycled aggregate concrete under uniaxial loading. Cement and Concrete Research. 2005;35:1187–1194. doi:10.1016/j.cemconres.2004.09.020.
3. Limbachiya MC, Leelawat T, Dhir RK. Use of recycled concrete aggregate in high-strength concrete. Materials and Structures. 2000;33:574–580. doi:10.1007/BF02480538.
4. Corinaldesi V, Moriconi G. Influence of mineral additions on the performance of 100% recycled aggregate concrete. Construction and Building Materials. 2009;23:2869–2876. doi:10.1016/j.conbuildmat.2009.02.004.
5. Tam VWY, Gao XF, Tam CM. Microstructural analysis of recycled aggregate concrete produced from two-stage mixing approach. Cement and Concrete Research. 2005;35:1195–1203. doi:10.1016/j.cemconres.2004.10.025.

6. Akhtar A, Sarmah AK. Construction and demolition waste generation and properties of recycled aggregate concrete: a global perspective. Journal of Cleaner Production. 2018;186:262–281. doi:10.1016/j.jclepro.2018.03.085.
7. Duan ZH, Kou SC, Poon CS. Prediction of compressive strength of recycled aggregate concrete using artificial neural networks. Construction and Building Materials. 2013;40:1200–1206. doi:10.1016/j.conbuildmat.2012.04.063.
8. Bu L, Du G, Hou Q. Prediction of the compressive strength of recycled aggregate concrete based on artificial neural network. Materials. 2021;14:3921. doi:10.3390/ma14143921.
9. Zhang X, Dai C, Li W, Chen Y. Prediction of compressive strength of recycled aggregate concrete using machine learning and Bayesian optimization methods. Frontiers in Earth Science. 2023;11:1112105. doi:10.3389/feart.2023.1112105.
10. Jagadesh P, Khan AH, Priya BS, et al. Artificial neural network and machine-learning modelling of compressive strength of recycled coarse aggregate based self-compacting concrete. PLoS ONE. 2024;19:e0303101. doi:10.1371/journal.pone.0303101.
11. Yang S, Sun J, Xu Z. Prediction on compressive strength of recycled aggregate self-compacting concrete by machine learning method. Journal of Building Engineering. 2024;88:109055. doi:10.1016/j.jobe.2024.109055.
12. Zhou X, Zhou J, Ohl JP. Improved prediction accuracy for compressive strength of recycled aggregate concrete using optimization-based algorithms and cascade forward neural network. Journal of Environmental Management. 2024;371:123068. doi:10.1016/j.jenvman.2024.123068.
13. Breiman L. Random forests. Machine Learning. 2001;45:5–32. doi:10.1023/A:1010933404324.
14. Chen T, Guestrin C. XGBoost: a scalable tree boosting system. Proceedings of the 22nd ACM SIGKDD International Conference on Knowledge Discovery and Data Mining. 2016:785–794. doi:10.1145/2939672.2939785.
15. Drucker H, Burges CJC, Kaufman L, Smola A, Vapnik V. Support vector regression machines. Advances in Neural Information Processing Systems. 1997;9:155–161.
16. Lundberg SM, Lee SI. A unified approach to interpreting model predictions. Advances in Neural Information Processing Systems. 2017;30:4765–4774.
17. Bureau of Indian Standards. IS 383: Specification for coarse and fine aggregates from natural sources for concrete. New Delhi, India.
18. Bureau of Indian Standards. IS 2386: Methods of test for aggregates for concrete; IS 10262: Concrete mix proportioning guidelines; IS 12269: 53 grade ordinary Portland cement. New Delhi, India.
19. Appendix A. Original Experimental Records
20. the original tabulated data and charts produced during the laboratory phase of this study are reproduced below
21. Figure A1. Original experimental record comprising the particle-size distribution, aggregate-property table, M30/M80 mixture tables, strength tables, and original bar charts.
22. Figure A2. Original experimental record comprising the Vee-Bee and slump tables and the original strength-loss and 28-day comparison charts.